Zygote

cambridge.org/zyg

Ultrastructural study: *in vitro* and *in vivo* differentiation of mice spermatogonial stem cells

Zahra Bashiri[1,2,3], Mansoureh Movahedin[4], Vahid Pirhajati[5], Hamidreza Asgari[1,2] and Morteza Koruji[1,2]

[1]Stem cell and Regenerative Medicine Research Center, Iran University of Medical Sciences, Tehran, Iran; [2]Department of Anatomy, School of Medicine, Iran University of Medical Sciences, Tehran, Iran; [3]Omid Fertility & Infertility Clinic, Hamedan, Iran; [4]Department of Anatomical Sciences, Medical Sciences Faculty, Tarbiat Modares University, Tehran, Iran and [5]Neuroscience Research Center, Iran University of Medical Sciences, Tehran, Iran

Research Article

Cite this article: Bashiri Z *et al.* (2024) Ultrastructural study: *in vitro* and *in vivo* differentiation of mice spermatogonial stem cells. *Zygote*. **32**: 87–95. doi: 10.1017/S096719942300062X

Received: 15 April 2023
Revised: 29 September 2023
Accepted: 23 November 2023
First published online: 27 December 2023

Keywords:
In vitro culture; Irradiation; Spermatogonia stem cells; Transplantation; Ultrastructure

Corresponding author:
Morteza Koruji; Email: koruji.m@iums.ac.ir

Summary

Mouse testicular tissue is composed of seminiferous tubules and interstitial tissue. Mammalian spermatogenesis is divided into three stages: spermatocytogenesis (mitotic divisions) in which spermatogonial stem cells (SSCs) turn into spermatocytes, followed by two consecutive meiotic divisions in which spermatocytes form spermatids. Spermatids differentiate into spermatozoa during spermiogenesis. Various factors affect the process of spermatogenesis and the organization of cells in the testis. Any disorder in different stages of spermatogenesis will have negative effects on male fertility. The aim of the current study was to compare the *in vitro* and *in vivo* spermatogenesis processes before and after transplantation to azoospermic mice using ultrastructural techniques. In this study, mice were irradiated with single doses of 14 Gy ^{60}Co radiation. SSCs isolated from neonatal mice were cultured *in vitro* for 1 week and were injected into the seminiferous tubule recipient's mice. Testicular cells of neonatal mice were cultured in the four groups on extracellular matrix-based 3D printing scaffolds. The transplanted testes (8 weeks after transplantation) and cultured testicular cells *in vitro* (after 3 weeks) were then processed for transmission electron microscopy studies. Our study's findings revealed that the morphology and ultrastructure of testicular cells after transplantation and *in vitro* culture are similar to those of *in vivo* spermatogenesis, indicating that spermatogenic cell nature is unaltered *in vitro*.

Introduction

Chemotherapy and radiotherapy cause damage to the spermatogonial stem cells (SSCs), which occupy a small part of the testes (Jahnukainen and Stukenborg, 2012). Irradiation of the testis has been shown to destroy spermatogonia, resulting in permanent azoospermia (Dym and Clermont, 1970; Kangasniemi *et al.*, 1990). Therefore, any disorder that leads to damage to SSCs at different stages of spermatogenesis can have negative effects on male fertility (Brinster, 2002). Spermatogenesis is a complex process of proliferation and differentiation of SSCs, during which SSCs change from diploid to haploid and gain fertility (Clermont, 1972). SSCs are undifferentiated germ cells located at the base of the basement membrane of seminiferous tubules attached to Sertoli cells. Sertoli cells are situated on the basal membrane of the tubules but have cytoplasmic ramifications throughout the epithelium up to the tubule lumen (Jégou, 1993). Sertoli cells play a crucial nursing role for germ cells and are believed to coordinate important events of spermatogenesis (Griswold, 1998).

SSCs have the ability to regenerate and differentiate into sperm and are the only cells in the body that are able to pass on genetic information to the next generation (Eslahi *et al.*, 2013). There is also a mixture of undifferentiated and differentiated spermatozoa in the testes of mice. Undifferentiated cells indicate SSC self-regeneration and continued spermatogenesis (Stukenborg *et al.*, 2008). In mice, A-single spermatogonia and committed progenitor spermatogonia (A-paired and A-aligned) together constitute undifferentiated spermatogonia (A-undiff; Chen and Liu, 2015). In the process of differentiation of spermatogonia (the process of differentiation can be seen from the A-paired stage), due to incomplete cytokinesis, cytoplasmic bridges are formed between spermatogonia (Ibtisham *et al.*, 2017). After the differentiation of committed cells begins, the first group of spermatogonia A differentiated A1 is created and forms A2 during mitotic division. A2 splits into A3 and A4. The next two divisions of mitosis make intermediate and B spermatogonia, respectively. B spermatogonia in mice enter the first meiotic division within 7–10 days and form primary spermatocytes. The meiotic process is long and lasts 13 days. After the first meiotic division, each primary spermatocyte produces two secondary spermatocytes. Round spermatids are the first stage after meiosis and

are not visible until days 20–21. It takes another 13 days for elongated spermatozoa to appear and the first mature sperm appears on day 35 (Ibtisham *et al.*, 2017).

Transplantation technology is a powerful tool to study the process of spermatogenesis that spermatogonia from a fertile donor mouse injected into the seminiferous tubules of an azoospermic model (Mohaqiq *et al.*, 2019). The first successful demonstration of spermatogonial cell transplantation was reported in 1994 (Brinster and Zimmermann, 1994). The donor spermatogonia was able to colonize the seminiferous tubules of the recipients and, in some cases, induce active spermatogenesis. Also, it has been used to assay the function of SSCs in transplanted germ cells in different species, including mice (Brinster and Avarbock, 1994; Brinster and Zimmermann, 1994), and primates (Avarbock *et al.*, 1996; Schlatt *et al.*, 2002). To enable the evaluation of the success of the transplantation, the recipient testes should have no or negligible endogenous spermatogenesis. Three-dimensional (3D) culture methods using scaffolds were investigated to provide favourable conditions for the behaviour of SSCs *in vitro* (Huleihel *et al.*, 2015). Scaffolds easily put the cell in contact with nutrients and oxygen and facilitate the excretion of waste products. According to studies, scaffolds play an important role in the proliferation and differentiation of SSCs (Eslahi *et al.*, 2013; Huleihel *et al.*, 2015). Also, in recent years, the extracellular matrix has been proposed as a biologically attractive material in biomedicine (Heydarkhan-Hagvall *et al.*, 2008). ECM provide many biological cues for cell migration, proliferation, and conduction/differentiation promotion and are widely used as biological materials for tissue engineering purposes (Fu *et al.*, 2014; Keane *et al.*, 2015). Although spermatogenesis after transplantation and on different culture systems may appear normal, this does not necessarily indicate that SSCs are functionally normal. The ideal test of sperm function is the successful production of offspring from the sperm generated after transplantation and sperm developed *in vitro*. The purpose of this study was to expand our previous study by investigating the ultrastructural changes of the differentiated testicular cells after transplantation and *in vitro* culture using ultrastructural and morphological techniques.

Materials and methods

The authors assert that all procedures contributing to this work comply with the ethical standards of the relevant national and institutional guides on the care and use of laboratory animals. The study ethics and protocols were approved by the Institutional Animal Care and Use Committee of the Iran University of Medical Sciences (Ethics code No. IR.IUMS.FMD.REC. 1400-1178).

Experimental animals for SSCs in vivo *and* in vitro *cultures*

For *in vivo* SSCs culture, male adult mice (age 6–8 weeks) from the National Medical Research Institute (NMRI), initially derived from original stocks obtained from Razi Laboratory (Tehran, Iran), were maintained under standard conditions with free access to food and water at the Animal Facilities of Iran University of Medical Sciences (Tehran, Iran). The research was conducted in accordance with National Research Council guidelines. The animals were kept in plastic cages in a room maintained at temperature range 22–25°C with a 12-h light/12-h dark cycle. The animals had free access to drinking water and standard laboratory pellets. The research was conducted in accordance with the National Research Council guidelines.

Testis irradiation

Animals were irradiated as described previously (Koruji *et al.*, 2008). In brief, animals were anaesthetized with a ketamine/xylazine (100 mg/kg:10 mg/kg) mixture before being radiated with ^{60}Co radiation from a cobalt therapy machine (Shohada-E-Tajrish Hospital). The dose rate was 1.37 Gy min^{-1}. The remainder of the body was shielded with lead plates. Mice were irradiated with single doses of 14 Gy. The crosswise application of tape to the lower abdomen prevented the mobilization of the testis to the scrotum. Irradiated and control animals were sacrificed by cervical dislocation 4 weeks after irradiation.

Germ cell collection, culture, and transplantation

The cells used were from a previous study for which a detailed methodology was published (Koruji *et al.*, 2009). Donor cells were isolated from the neonate mouse testis. After *in vitro* culture, SSCs were transplanted into the seminiferous tubules of the adult mouse testis, which were irradiated with 14 Gy ^{60}Co radiation from a cobalt therapy machine (Shohada-E-Tajrish Hospital) at 10 weeks of age, by the rete testis. The irradiated recipients were devoid of endogenous spermatogenesis at the time of transplantation (4 weeks after radiation treatment) (Koruji *et al.*, 2008). The adult recipient mice were anaesthetized using ketamine/xylazine (100 mg/kg:10 mg/kg) mixture (Alfasan, Woerden, The Netherlands). In total, 10^5 of the donor SSCs in 10 µl Dulbecco's modified Eagle's medium (DMEM) were injected into the seminiferous tubules in one of the testes of the recipient mouse. The transplanted mouse testis was examined 8 weeks after transplantation for ultrastructural study.

SSC culture on a 3D system in vitro

Testicular extracellular matrix (ECM) extraction

Testicular tissue was decellularized as described previously (Bashiri *et al.*, 2021). Testis from five 1-year-old rams were obtained from a local slaughterhouse, and testicular tissue fragments were decellularized in 3.4 M NaCl buffer for 30 min and then in Triton X-100 solution (0.1%) for 15 min before being solubilized in urea extraction (Bashiri *et al.*, 2021). The extracted ECM was then lyophilized using a freeze dryer and stored at −20°C.

Preparation of the bio-ink and 3D printing of the scaffolds

According to our previous study (Bashiri *et al.*, 2021, 2022), testicular tissue ECM powder (5%) was dissolved in 1 ml of DMEM (Gibco) for 48 h with a magnetic stirrer. The ECM solution (5% w/v) was combined with the alginate–gelatin solution (6%:6%). The scaffolds were printed (3DPL, Iran) according to parameters including pressure of 1/1 bar, temperature of 25°C, dimensions of 7 mm × 0.15 mm, strand distance of 1.3 mm, and strand thickness of 2 mm. Then printed structures were cross-linked using 300 mM calcium chloride ($CaCl_2$, anhydrous, granular, ≥ 7.0 mm, ≥ 93.0%) and 0.25% glutaraldehyde (814393, Merck, USA) for 15 min and washed for 30 min. Scaffolds were printed in the following two groups:

1. Hybrid scaffolds: obtained from alginate–gelatin solution and ECM solution (0%).
2. Composite scaffolds: obtained from alginate–gelatin solution and ECM solution (5%).

Isolation of mouse SSCs

Testes of neonate mice were collected for the preparation of cell suspension following enzymatic digestion and purification steps.

https://doi.org/10.1017/S096719942300062X Published online by Cambridge University Press

Testicular cells were separated by the method of Van Pelt *et al.* (1996) with minor modifications. Briefly, minced testis pieces were suspended in DMEM containing 0.5 mg/ml collagenase/dispase, 0.5 mg/ml trypsin, and 0.05 mg/ml DNase for 30 min (with shaking and a little pipetting) at 37°C. All enzymes were purchased from Sigma-Aldrich. As a result, testicular cells [testicular suspension containing spermatogonia, Sertoli, and peritubular cells (Leydig and myoid)] were obtained after the first enzymatic digestion. A second digestion step was performed in DMEM by adding a fresh enzyme solution into the seminiferous cord fragments as described above. As a result, spermatogonia and Sertoli cells were obtained after the second enzymatic digestion. The collected cells were used for the culture cells.

SSC differentiation on 3D printing scaffolds

After sterilization of hydrogel scaffolds using ultraviolet (UV) light, the scaffolds were placed in a culture medium containing 10% knock-out serum replacement (KSR; 10828028, Gibco) and 1% penicillin–streptomycin in 24-well plates for 24 h. We used non-treated cell culture plates so that the cells would not attach to the bottom of the plate but only to the scaffold. Then, before seeding the cells, the culture medium was removed from the scaffolds, and ~50 λ cell suspension containing $10^5 \times 3$ cells were loaded onto the printed scaffolds. The number of cells was determined using a haematocytometer. After 3 h of cell adhesion on the scaffold surface, ~0.5 ml of differentiation medium [DMEM/F12 containing M6 10 × 2 retinoic acid (R2625; Sigma-Aldrich), 5 IU/l follicle-stimulating hormone (FSH; Gonal-F, Merck), 5 IU/l human chorionic gonadotropin (hCG; Choriomon, Switzerland), and 40 ng/ml BMP4], containing 10% KSR and 1% penicillin–streptomycin were added to the cells. Half of the culture medium was exchanged every other day. Mouse SSCs were cultured for 3 weeks in the following four groups:

Group 1: SSCs co-cultured with Sertoli cells on an alginate–gelatin hybrid scaffold,

Group 2: SSCs co-cultured with Sertoli cells on an ECM–alginate–gelatin composite scaffold,

Group 3: Culture of testicular cells on an alginate–gelatin hybrid scaffold,

Group 4: Culture of testicular cells on an ECM–alginate–gelatin composite scaffold.

3D printed scaffolds, tissue collection, processing, and electron microscopic study

3D printed scaffolds and mouse testes (NMRI) were perfusion fixed according to the technique of Sprando (1990). In brief, normal saline was perfused initially to clear the blood from the testes, followed by 5% (w/v) glutaraldehyde (pH 7.2–7.4) and 4% paraformaldehyde. After glutaraldehyde perfusion of ~20 min, the testes were excised and fixed in 2.5% glutaraldehyde in phosphate-buffered saline (PBS; pH 7.4) for 2 h, and postfixed with 1% osmium tetroxide in the same buffer for 2 h. After dehydration in an ascending series of ethanol, specimens were placed in propylene oxide and embedded in Epon 812 (TAAB, UK). Semi-thin sections (0.5 mm) were stained with toluidine blue for light microscopy. Transmission electron microscopy (TEM; Zeiss EM 900, Germany) was used to look at ultrathin sections (60–80 nm) that had been stained with uranyl acetate and lead citrate.

Results

Ultrastructural features of seminiferous tubules and germ cells in normal mice

In normal testes, all cell lines were observed, and all cells showed normal characteristics (Figure 1). Examining the electron microscope sections showed that SSCs (Figure 1A–C) are located individually at the base of the seminiferous tubule. Spermatogonia cell shapes varied from a pear-shaped cell containing a round nucleus to a flat cell containing an elongated nucleus. The shape of the spermatogonia nucleus is usually homogeneous and the nucleoplasm is slightly granular. These cells have a spotted appearance due to the heterochromatin of the nucleus around the membrane. The ratio of nucleus to cytoplasm in these cells was high, and there was a reticular nucleolus near the centre of the nucleus. The most important organelle of the cytoplasm is relatively large mitochondria, which are often seen in the clusters around the nucleus. In addition, the images showed moderate amounts of free ribosomes.

Sertoli cells (Figure 1A,C) are also located near SSCs and have an irregular appearance and nucleus. The nucleus in these cells was jagged and had deep depressions, and scattered heterochromatin spots were seen. Small and spherical mitochondria with blade-like stigmas and lipid inclusions were observed in their cytoplasm. Sertoli cells with numerous cytoplasmic protrusions surround the developing cell lines. Leydig cells in the testis tissue have an ovoid nucleus and euchromatin, and their cytoplasm contains abundant mitochondria and lipid droplets (Figure 1D). Small parts of the synaptonemal complex were seen in the nucleus of the spermatocyte cell (Figure 1C). Also, elongated mitochondria with large and open cisternae, which are a prominent feature of these cells, were abundantly visible in the cytoplasm. Spermatid cells are smaller than spermatocyte cells and are close to the luminal space, and acrosomal vesicles were also seen forming (Figure 1E,F). Elongating spermatids are characterized by long heads, the flagellum is forming, and the mitochondria are moving towards the tail (Figure 1F–H). Sperm was also identified with elongated nuclei and acrostic sacs (Figure 1H,I).

Ultrastructure study of testicular cells after gamma irradiation

The ultrastructure of SSCs in testicular tissue was examined after gamma irradiation and after cell transplantation using TEM microscopy. At 4 weeks after irradiation, the seminiferous tubules were free of germ cells, and spermatogonia were rarely present at the base of the tube. The presence of large vacuoles in the tube was observed due to the loss of germ cells after irradiation. Another characteristic of Sertoli cells after irradiation was the presence of many vacuoles of different sizes and shapes in the cytoplasm. These vacuoles appear to be electron-transparent vesicles of various sizes, lacking a defined morphological content and closely related to normal tubules or other vesicles. A comparison of the ultrastructure of spermatogonia 4 weeks after irradiation did not show any difference with cells in normal tubes (Figure 2).

Ultrastructure study of transplanted cells into recipient mice's testis

The ultrastructure of SSCs was evaluated after cell transplantation. After transplantation, cell lines were observed again, and all cells

https://doi.org/10.1017/S096719942300062X Published online by Cambridge University Press

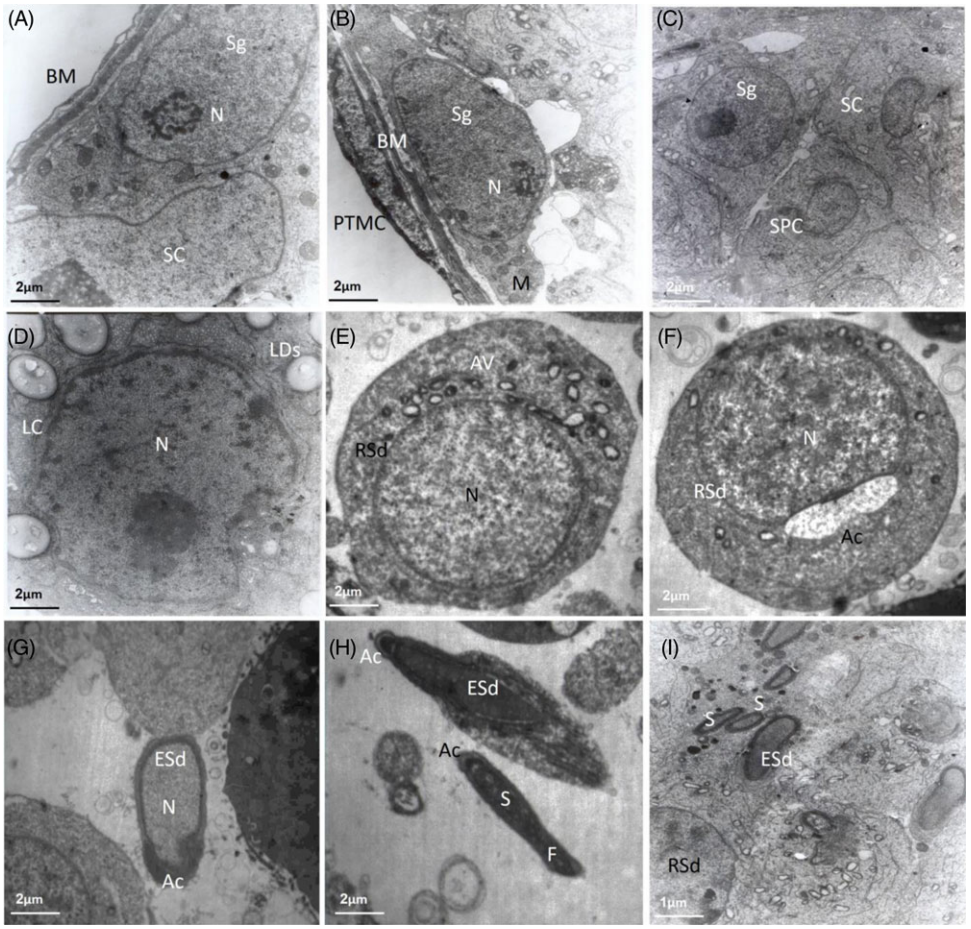

Figure 1. TEM images (A-I) of testicular tissue in normal mice. Different germ cell lines (morphologic transformation of the germ cell to sperm) was observed. Abbreviations: nucleus (N), mitochondria (M), rough endoplasmic reticulum (RER), basement membrane (BM), peritubular myoid cells (PTMCs), Leydig cells (LC), lipid droplets (LDs), acrosome vesicles (AV), Sertoli cells (SC), spermatogonia (Sg), spermatocytes (SPC), round spermatids (RSd), elongated spermatids (ESd), acrosome (Ac), sperm tail (F), sperm (S).

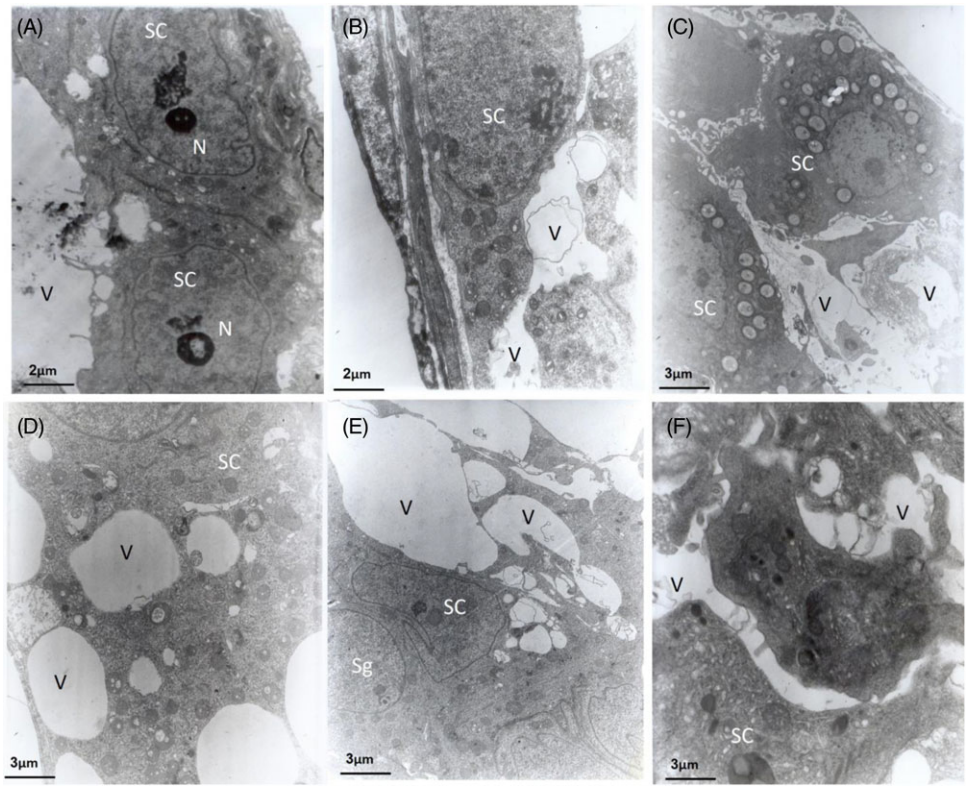

Figure 2. (A–F) TEM images of mice testicular tissue after gamma irradiation. At 4 weeks after irradiation, large vacuoles are seen in the tube due to the loss of germ cells. Abbreviations: nucleus (N), Sertoli cells (SC), spermatogonia (Sg), vacuoles (V).

https://doi.org/10.1017/S096719942300062X Published online by Cambridge University Press

showed normal characteristics (Figure 3). A comparison of the ultrastructure of cells after transplantation did not show any difference from cells in normal tubes.

Ultrastructure of differentiated cells on printed scaffolds

The results of our study showed that, in groups 1 and 3, cells were found in the stages of spermatogonia, spermatocytes, and spermatids (Figure 4A–C,I–K). In group 2, differentiated cells including spermatocytes, and different stages of spermatids, including round, elongating, and elongated spermatids, were observed (Figure 4E–G). In group 4, mature sperm ultrastructure, including an elongated head shape and long flagella-like appendages, was visible (Figure 4M–O). SCs had large spherical nuclei with one or two prominent nucleoli located along the nuclear membrane or in the centre of the nucleus. The spherical nucleus consisted of scattered heterochromatin shells in SCs. The nucleus had a prominent, irregularly shaped nucleolus that occupied an unusual position in the nucleus. The cytoplasm was characterized by organs such as relatively large numbers of globular mitochondria, rough endoplasmic reticulum, and vesicles that were mostly located in the perinuclear region (Figure 4A). Primary spermatocytes have a perfectly round nucleus and prominent mitochondria in the cytoplasm, and are found in the pachytene-prophase stage. Secondary spermatids are not much different from primary spermatocytes, but they are smaller cells with a high chromatin density, which occurs from the outside to the inside (Figure 4B,I). On the scaffolds, three developmental phases of spermatids were identified: Round spermatids (Golgi phase) are often associated with the emergence of quasistellar Golgi, which appears to ultimately contribute to acrosome formation. Round to ovoid spermatids represent the formation of acrosomes (cap phase). Many microtubules are associated with the Golgi phase as well as the acrosome (Figure 4E,F,J). During the spermatid elongation phase, a simple or primary strand of microtubules forms beneath the perinuclear ring. Secondary spermatids are characterized by long heads and a caudal tube (posterior part of the manchette) at the posterior part of the head. The spermatid nucleus is located on one side, and in some spermatids, the flagellum forms and the mitochondria move towards the tail (Figure 4C,G,K). However, mature sperm had low cytoplasm and the nucleus was denser. Mitochondria were observed in the middle of the tail in longitudinal sections and axon microtubules in cross-sections (Figure 4M–O). Sertoli cells have a jagged nucleus with deep depressions and scattered heterochromatin spots. Large and spherical mitochondria with blade-like stigmas and lipid inclusions were observed in their cytoplasm. The number of vacuoles in the Sertoli cells of the culture system was slightly higher than that of the testicular tissue. (Figure 4D,L). The results of studies using the TEM technique showed that Leydig cells are spherical cells with an ovoid nucleus and euchromatin, and their cytoplasm contains abundant mitochondria and numerous lipid vesicles (Figure 4H,P). The results showed that although many various types of spermatogonia were identified, no marked difference was observed between spermatogonial cells in the culture system and testis tissue. There was no evidence of changes in the morphology of spermatogonial cells or damage in the mitochondria, nucleus and other organelles of Sertoli cells compared with the testis tissue, which indicates that these cells were well preserved in the culture system.

Discussion

Male germ cells arise from stem cell stores located at the basement membrane of the seminiferous tubule. Spermatogenesis is a complex but highly coordinated process that is regulated by paracrine, autocrine, and juxtacrine pathways between the cell germ, somatic cells, and endocrine glands (Chocu *et al.*, 2012). In the mature testis, mouse SSCs comprise a small cell population (0.03%), similar to other stem cells. The reason for this small number is that SSCs enter differentiation quickly. The spermiogenesis process includes a series of biochemical, cytochemical, and structural modifications (Amaral *et al.*, 1999), including chromatin density, acrosome formation, mitochondrial sheath formation in the middle, shrinkage of the cytoplasm with the removal of residual bodies, and flagellum formation (Cheng and Mruk, 2009). Therefore, mature sperm are released from Sertoli cells of the seminiferous tubules as elongated cells with a head that includes the nucleus and acrosome and a tail or flagellum (Fawcett, 1975). The natural structure of sperm in all species can affect the functional aspects of fertilization events and, subsequently, embryo formation. Age, fertility lifespan, radiation exposure, and chemical nanoparticles (Thakur *et al.*, 2014) are variables that may have an effect on sperm organization in the testis (Ramm *et al.*, 2014). In this study, we used ultrastructural techniques to examine testicular cells after transplantation and *in vitro* culture. In 1952, Watson (1952) conducted the first ultrastructural investigation of spermatogenesis using electron microscopy. After that, numerous research studies have analyzed the morphology and ultrastructure of sperm and spermiogenesis in various species (Lan *et al.*, 1999; Xianjiang and Suo, 2000; Tudge *et al.*, 2001; Medina *et al.*, 2006; Kang *et al.*, 2008; Villagra *et al.*, 2018; van der Horst *et al.*, 2019). This study examined the structural changes that occurred in mouse testicular cells during the spermatogenesis of a normal testis. Classifying spermatogenesis according to the level of cell differentiation is necessary for the evaluation of complicated morphological changes in testicular epithelial cells.

Based on the relative amount of heterochromatin covering the nucleus and the cytoplasmic organ accumulations, our evaluation criteria for cell identification were developed. SSCs were discovered in the basal layer of the seminiferous epithelium, and their attachment to the basement membrane served as our primary indicator for distinguishing spermatogonia from spermatocytes. Their nuclei contained uniform chromatin and pale nucleoplasm. The findings of this study demonstrate that the amount of heterochromatin covering the nucleus in spermatogonia increased as the cells divided, and that the shape of the cells changed or organs in the cytoplasm moved around because of pressure from the surrounding cells (Chiarini-Garcia and Russell, 2002).

Primary spermatocytes are clearly identified, and some of them have intercellular bridges. Most cells seen are in the first prophase of mitotic division, which lasts ~22 days and is distinguished by the presence of chromosomes in various states of colliding in their nucleus. It is challenging to observe secondary spermatocytes in histological sections because they are smaller than primary spermatocytes and have fewer membrane complexes. In the testis of normal mice, three stages of spermatids were detected, which indicates that this gradual morphological difference of the spermatid is required to classify the stages of spermiogenesis. Round spermatids had spherical nuclei, and proacrosomal aggregations and acrosomal granules were visible at this stage. The elongating spermatid had an enlarged nucleus, and the tails were free in the lumen of a transparent caudal tube (the posterior

https://doi.org/10.1017/S096719942300062X Published online by Cambridge University Press

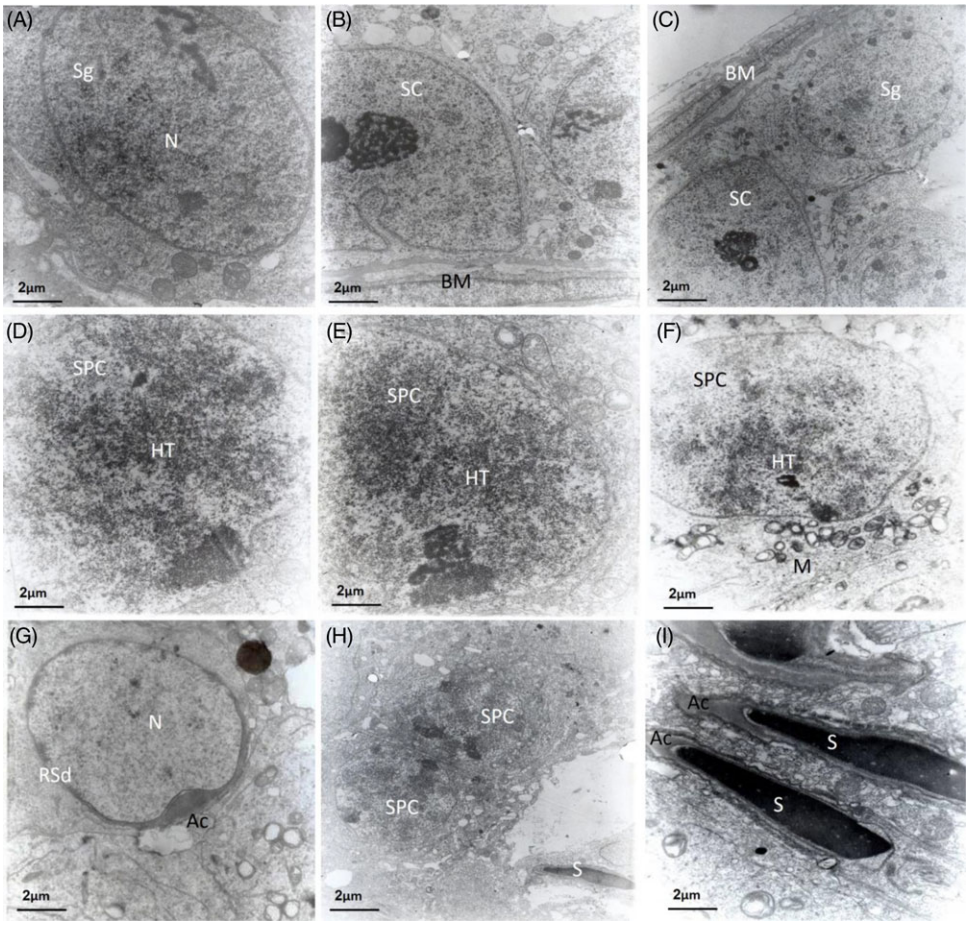

Figure 3. (A–I) TEM images of mice testicular tissue 8 weeks after autologous transplantation. Abbreviations: nucleus (N), basement membrane (BM), heterochromatin (Ht) regions, acrosome vesicles (AV), Sertoli cells (SC), spermatogonia (Sg), spermatocytes (SPC), round spermatids (RSd), acrosome (Ac), sperm (S).

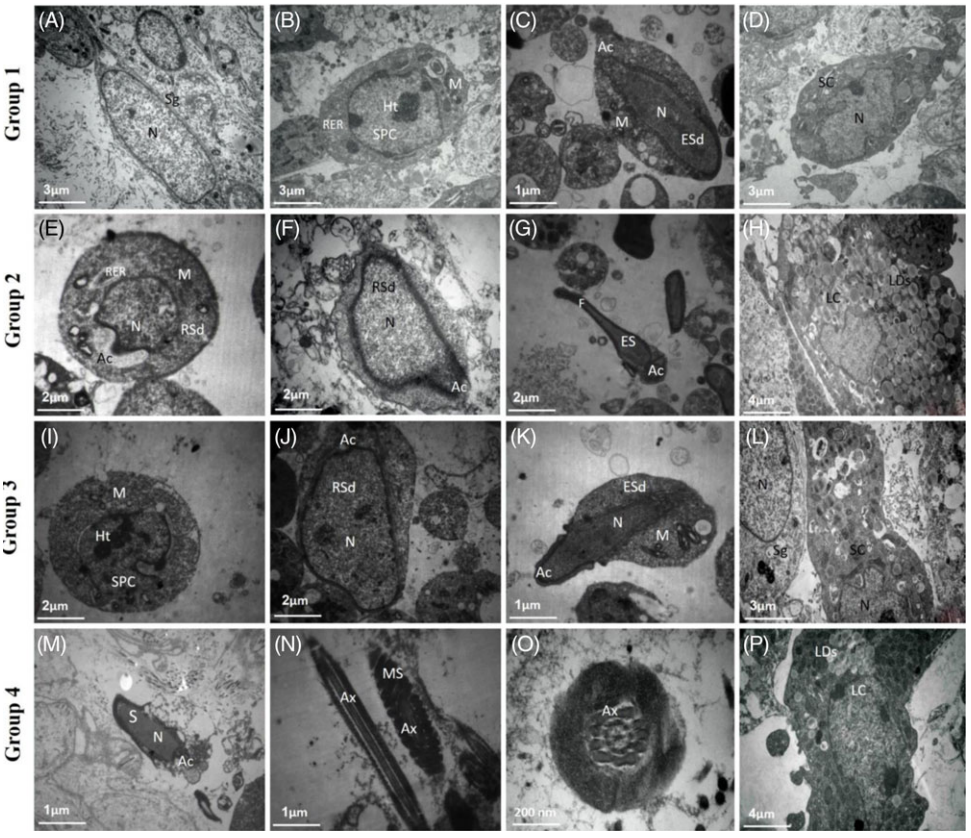

Figure 4. (A–P) Ultrastructure of testicular cells *in vitro* after the differentiation period. Sections of TEM showed that cells derived from SSC colonies indicated distinct morphology of differentiated cells *in vitro*. Spermatogonia (Sg), nucleus (N), mitochondria (M), rough endoplasmic reticulum (RER), nucleus (Nu), heterochromatin (Ht) regions, spermatocytes (SPC), Leydig cells (LC), lipid droplets (LDs), Sertoli cells (SC), round spermatids (RSd), elongated spermatids (ESd), acrosome (Ac), sperm tail (F), sperm (S), axoneme (Ax), mitochondrial sheath (MS).

https://doi.org/10.1017/S096719942300062X Published online by Cambridge University Press

section of the manket) that emerged at the back of the spermatid's head. Although the appearance and structure of sperm vary between species, they all have the same features, such as compact nuclei and flagella. In the testes of normal mice, sperm were observed to have a normal structure with a normal head shape, a healthy plasma membrane, acrosomes, and homogeneous nuclei.

During the course of cancer treatment, ionizing radiation and chemical substances may result in defects in spermatogenesis (Somosy, 2000) and permanent or long-term infertility (Izadyar *et al*., 2000). Testicular cell transplantation has been widely used to investigate the regeneration of spermatogenesis in various species (Rodriguez-Sosa and Dobrinski, 2009). In the current study, we investigated the extent of changes in the structure of the mouse testis after radiation. Examining the testes in the radiation group indicated that most of the tubules lack germ cells and contain only one basic row of nuclei. Our observations also showed that radiation decreased the diameter of the testis and the lumen, and this change was probably caused by the loss of SSCs (Creemers *et al*., 2002; Koruji *et al*., 2008), but it did not impair the function of Leydig and Sertoli cells to support spermatogenesis. Our study's findings are in line with those of other studies (Kashiwabara *et al*., 2003; Kim *et al*., 2006).

A previous light microscope study presented numerous quantitative and qualitative parameters related to SSC transplants (Parreira *et al*., 1998; Koruji *et al*., 2008). The present study extends these findings to the ultrastructural level. The study also utilizes morphometric techniques to demonstrate that the testis weight increase beginning at 24 h post-transplantation is due to an increase in the size of the tubular lumen.

The results of the research showed that the administration of chemicals harms the Sertoli cells and triggers the formation of numerous vacuoles within them. These vacuoles may be formed in the basal Sertoli cell cytoplasm (microvacuolation). Another type of vacuolization (macrovacculation) is observed in the depth of the seminiferous epithelium, which may indicate the expansion of the endoplasmic reticulum or the intercellular spaces containing fluid or lipids. Additionally, vacuoles may also appear within or between Sertoli cells. Vacuoles between Sertoli cells may represent spaces representing germ cell degeneration/atrophy. These gaps confirm the loss of germ cells in testicular tissue after injury (Mirzapour *et al*., 2017). In one study, empty spaces containing lipid droplets were formed in Sertoli and Leydig cells, and symptoms of testicular inflammation were observed using nanomaterials (Shokri *et al*., 2012). In another study, treatment with ethane dimethane sulfonate (EDS) caused degeneration of germ cells and the formation of numerous vacuoles and intercellular spaces in Sertoli cells. Many morphological changes have been observed at the Sertoli cell junction (Kerr *et al*., 1993).

In the present study, electron microscopic findings in the testes of irradiated mice showed that the ultrastructure of the remaining spermatogonia was similar to that of the normal testis. Conversely, large vacuoles in the cytoplasm of Sertoli cells indicate a suitable space for transplanted cells. The ultrastructure examination of the transplanted testis and its comparison with normal testicular cells did not show any difference that indicates the presence of a suitable testicular microenvironment for transplantation. The use of topical radiation at the appropriate dose to prepare the recipient models in mice, rats, and cattle was confirmed in various studies.

Most studies have discussed *in vivo* spermatogenesis in various species, and few research studies have investigated *in vitro* spermatogenesis. There are limited studies about the effects of culture medium and *in vitro* culture on the ultrastructural properties of SSCs. These effects have not yet been fully elucidated and need to be investigated. According to studies, stem cells are vulnerable to stress and run a higher risk of alteration when exposed to differentiation or growth stimuli *in vitro* (enzymatic digestion, pH changes, and unknown factors). Kanatsu-Shinohara *et al.* (2005) demonstrated that mouse SSCs did not change after 2 years of culture *in vitro*, and after transplantation of these cells, the derived sperm were used for ICSI and produced offspring. However, it has been seen the offspring obtained from mouse SSCs cultured *in vitro* are normal. Our ultrastructure results prove that there is no difference between produced sperm after transplantation.

In rodents and humans, the relative quantity of heterochromatin nuclei detected by the nucleus is a specific feature of spermatogonia (Russell *et al*., 1993). According to previous studies, the primary spermatogonia (As, Apr, and Aal) show a large nucleus relative to the cytoplasm, in which the nucleus and regions of heterochromatin had lower density, while the appearance of heterochromatin increased in the differentiating SSCs (Bellvé *et al*., 1977; Eslahi *et al*., 2013). Gerton and Millette (1984) isolated round spermatids from adult mouse testis and incubated them in DMEM culture medium in the presence or absence of demecolcine. Their findings using the TEM technique indicated that round spermatids with flagellum-like structures were observed in the demecolcine-without group after 24 h of incubation. These structures might be recognized by their non-random rotational motions and uniform thickness along their length. They displayed normal structures with plasma membranes surrounding the $2+9$ microtubular axonemes. Eslahi *et al.* (2013) cultured mouse SSCs on PLLA nanofibre scaffolds and discovered cells with morphology similar to SSCs, including heterochromatin-rich nuclei, a rough endoplasmic reticulum, and many mitochondria surrounding the nucleus (Eslahi *et al*., 2013). The progression of spermatogenesis and differentiated structures on the 3D-printed scaffolds were also confirmed using TEM microscopy. According to the results of this technique, the highest degree of differentiation was observed in group 4, so the structure of these cells in group 4 is quite similar to mature sperm with a specialized structure. The tail consists of 9+2 microtubular axonemes, dense external fibres, a mitochondrial helix, a longitudinal column of fibrous sheath, and a plasma membrane around the cell. In group 2, different stages of spermatids with intact ultrastructure were observed. In groups 1 and 3, differentiated cells up to the stage of secondary spermatocytes, round and elongating spermatids were observed.

Secondary spermatocytes differ from primary spermatids in that they are smaller and have higher chromatin densities than primary spermatids. The condensing spermatid nucleus is on one side. Primary spermatocytes have completely elliptical nuclei and prominent mitochondria in the cytoplasm. Although primary spermatids are smaller cells with a higher chromatin density than secondary spermatocytes, they do not differ significantly from them. The round spermatid nucleus is located on one side and has more density. The elongating spermatid nucleus is denser, and the mitochondria are located in the middle, occupying half of the head in the elongated sperm. To our knowledge, *in vitro* maturation of Leydig cells in neonatal testis cells has not yet been reported. In the present study, the presence of numerous cytoplasmic lipid droplets in Leydig cells was observed in group 4, indicating that these cells were able to mature *in vitro* after 3 weeks of culture and maintain their function in response to gonadotropins (Cham *et al*., 2021). Our findings revealed that, in group 4, there was complete

https://doi.org/10.1017/S096719942300062X Published online by Cambridge University Press

differentiation of SSCs up to the sperm stage but, in other groups, the differentiation was not complete. It can be concluded that there is not much difference between the morphology of cultured cells on printed ECM-based systems and *in vivo*, which can provide ideal conditions for the differentiation of SSCs similar to seminiferous tubules in normal testis. More investigation is needed to determine sperm functionality. This result indicated that the culture system probably did not alter the structure of spermatogonial cells. However, significant efforts are required to accurately identify these cells at the protein and molecular level prior to transplantation.

In conclusion, various factors affect the process of spermatogenesis and the organization of cells in the testis. Any disorder in different stages of spermatogenesis will have negative effects on male fertility. The results showed that the seminiferous tubules were free of germ cells after irradiation, and spermatogonia were rarely present at the base of the tube. Also, large vacuoles were observed in the testis tubules. Our findings revealed that the ultrastructure of testicular cells after transplantation and *in vitro* culture was similar to that of *in vivo* spermatogenesis, indicating that the nature of spermatogenic cells was unaltered *in vitro*. More effort is needed to investigate the morphology and ultrastructure of germ cells *in vitro* and *in vivo* for diagnostic and clinical purposes.

Data availability. Data will be made available on request. All data generated or analyzed during this study are included in this published article.

Acknowledgements. This study was funded by grants from the Iran National Science Foundation (INSF, 4004177) and the Iran University of Medical Sciences (IUMS, 1400-1178).

Author contributions. Zahra Bashiri: Investigation; Methodology; Writing – original draft. Mansoureh Movahedin and Hamireza Asgari: Conceptualization; Writing – review and editing. Vahid Pirhajati: TEM, Software; Resources; Visualization. Morteza Koruji: Conceptualization; Project administration; Resources; Writing – review and editing.

Competing interests. The authors have no conflict of interest to declare.

References

Amaral, M. J., Fernandes, A. P., Báo, S. N. and Recco-Pimentel, S. M. (1999). An ultrastructural study of spermiogenesis in three species of *Physalaemus* (Anura, Leptodactylidae). *Biocell*, **23**(3), 211–221.

Avarbock, M. R., Brinster, C. J. and Brinster, R. L. (1996). Reconstitution of spermatogenesis from frozen spermatogonial stem cells. *Nature Medicine*, **2**(6), 693–696. doi: 10.1038/nm0696-693

Bashiri, Z., Amiri, I., Gholipourmalekabadi, M., Falak, R., Asgari, H., Maki, C. B., Moghaddaszadeh, A. and Koruji, M. (2021). Artificial testis: Testicular tissue extracellular matrix as a potential bio-ink for 3D printing. *Biomaterials Science*, **9**(9), 3465–3484. doi: 10.1039/d0bm02209h

Bashiri, Z., Gholipourmalekabadi, M., Falak, R., Amiri, I., Asgari, H., Chauhan, N. P. S. and Koruji, M. (2022). *In vitro* production of mouse morphological sperm in artificial testis bioengineered by 3D printing of extracellular matrix. *International Journal of Biological Macromolecules*, **217**, 824–841. doi: 10.1016/j.ijbiomac.2022.07.127

Bellvé, A. R., Cavicchia, J. C., Millette, C. F., O'Brien, D. A., Bhatnagar, Y. M. and Dym, M. (1977). Spermatogenic cells of the prepuberal mouse: Isolation and morphological characterization. *Journal of Cell Biology*, **74**(1), 68–85. doi: 10.1083/jcb.74.1.68

Brinster, R. L. (2002). Germline stem cell transplantation and transgenesis. *Science*, **296**(5576), 2174–2176. doi: 10.1126/science.1071607

Brinster, R. L. and Avarbock, M. R. (1994). Germline transmission of donor haplotype following spermatogonial transplantation. *Proceedings of the National Academy of Sciences of the United States of America*, **91**(24), 11303–11307. doi: 10.1073/pnas.91.24.11303

Brinster, R. L. and Zimmermann, J. W. (1994). Spermatogenesis following male germ-cell transplantation. *Proceedings of the National Academy of Sciences of the United States of America*, **91**(24), 11298–11302. doi: 10.1073/pnas.91.24.11298

Cham, T. C., Ibtisham, F. I., Fayaz, M. A. and Honaramooz, A. (2021). Generation of a highly biomimetic organoid, including vasculature, resembling the native immature testis tissue. *Cells*, **10**(7), 1696. doi: 10.3390/cells10071696

Chen, S.-R. and Liu, Y.-X. (2015). Regulation of spermatogonial stem cell self-renewal and spermatocyte meiosis by Sertoli cell signaling. *Reproduction*, **149**(4), R159–R167. doi: 10.1530/REP-14-0481

Cheng, C. Y. and Mruk, D. D. (2009). An intracellular trafficking pathway in the seminiferous epithelium regulating spermatogenesis: A biochemical and molecular perspective. *Critical Reviews in Biochemistry and Molecular Biology*, **44**(5), 245–263. doi: 10.1080/10409230903061207

Chiarini-Garcia, H. and Russell, L. D. (2002). Characterization of mouse spermatogonia by transmission electron microscopy. *Reproduction*, **123**(4), 567–577. doi: 10.1530/rep.0.1230567

Chocu, S., Calvel, P., Rolland, A. D. and Pineau, C. (2012). Spermatogenesis in mammals: Proteomic insights. *Systems Biology in Reproductive Medicine*, **58**(4), 179–190. doi: 10.3109/19396368.2012.691943

Clermont, Y. (1972). Kinetics of spermatogenesis in mammals: Seminiferous epithelium cycle and spermatogonial renewal. *Physiological Reviews*, **52**(1), 198–236. doi: 10.1152/physrev.1972.52.1.198

Creemers, L. B., Meng, X., Den Ouden, K., Van Pelt, A. M. M., Izadyar, F., Santoro, M., Sariola, H. and De Rooij, D. G. (2002). Transplantation of germ cells from glial cell line-derived neurotrophic factor-overexpressing mice to host testes depleted of endogenous spermatogenesis by fractionated irradiation. *Biology of Reproduction*, **66**(6), 1579–1584. doi: 10.1095/biolreprod66.6.1579

Dym, M. and Clermont, Y. (1970). Role of spermatogonia in the repair of the seminiferous epithelium following X-irradiation of the rat testis. *American Journal of Anatomy*, **128**(3), 265–282. doi: 10.1002/aja.1001280302

Eslahi, N., Hadjighassem, M. R., Joghataei, M. T., Mirzapour, T., Bakhtiyari, M., Shakeri, M., Pirhajati, V., Shirinbayan, P. and Koruji, M. (2013). The effects of poly L-lactic acid nanofiber scaffold on mouse spermatogonial stem cell culture. *International Journal of Nanomedicine*, **8**, 4563–4576. doi: 10.2147/IJN.S45535

Fawcett, D. W. (1975). The mammalian spermatozoon. *Developmental Biology*, **44**(2), 394–436. doi: 10.1016/0012-1606(75)90411-x

Fu, R. H., Wang, Y.-C. W., Liu, S.-P., Shih, T.-R., Lin, H.-L., Chen, Y.-M., Sung, J.-H., Lu, C.-H., Wei, J. R., Wang, Z.-W., Huang, S. J., Tsai, C. H., Shyu, W. C. and Lin, S. Z. (2014). Decellularization and recellularization technologies in tissue engineering. *Cell Transplantation*, **23**(4–5), 621–630. doi: 10.3727/096368914X678382

Gerton, G. L. and Millette, C. F. (1984). Generation of flagella by cultured mouse spermatids. *Journal of Cell Biology*, **98**(2), 619–628. doi: 10.1083/jcb.98.2.619

Griswold, M. D. (1998). The central role of Sertoli cells in spermatogenesis. *Seminars in Cell and Developmental Biology*, **9**(4), 411–416. doi: 10.1006/scdb.1998.0203

Heydarkhan-Hagvall, S., Schenke-Layland, K., Dhanasopon, A. P., Rofail, F., Smith, H., Wu, B. M., Shemin, R., Beygui, R. E. and MacLellan, W. R. (2008). Three-dimensional electrospun ECM-based hybrid scaffolds for cardiovascular tissue engineering. *Biomaterials*, **29**(19), 2907–2914. doi: 10.1016/j.biomaterials.2008.03.034

Huleihel, M., Nourashrafeddin, S. and Plant, T. M. (2015). Application of three-dimensional culture systems to study mammalian spermatogenesis, with an emphasis on the rhesus monkey (*Macaca mulatta*). *Asian Journal of Andrology*, **17**(6), 972–980. doi: 10.4103/1008-682X.154994

Ibtisham, F., Wu, J., Xiao, M., An, L., Banker, Z., Nawab, A., Zhao, Y. and Li, G. (2017). Progress and future prospect of *in vitro* spermatogenesis. *Oncotarget*, **8**(39), 66709–66727. doi: 10.18632/oncotarget.19640

Izadyar, F., Creemers, L. B., van Dissel-Emiliani, F. M., van Pelt, A. M. and de Rooij, D. G. (2000). Spermatogonial stem cell transplantation. *Molecular and Cellular Endocrinology*, **169**(1–2), 21–26. doi: 10.1016/s0303-7207(00)00346-4

Jahnukainen, K. and Stukenborg, J.-B. (2012). Clinical review: Present and future prospects of male fertility preservation for children and adolescents. *Journal of Clinical Endocrinology and Metabolism*, **97**(12), 4341–4351. doi: 10.1210/jc.2012-3065

Jégou, B. (1993). The Sertoli-germ cell communication network in mammals. *International Review of Cytology*, **147**, 25–96. doi: 10.1016/S0074-7696(08)60766-4

Kanatsu-Shinohara, M., Ogonuki, N., Iwano, T., Lee, J., Kazuki, Y., Inoue, K., Miki, H., Takehashi, M., Toyokuni, S., Shinkai, Y., Oshimura, M., Ishino, F., Ogura, A. and Shinohara, T. (2005). Genetic and epigenetic properties of mouse male germline stem cells during long-term culture. *Development*, **132**(18), 4155–4163. doi: 10.1242/dev.02004

Kang, X., Ge, S., Guo, M., Liu, G. and Mu, S. (2008). A transmission electron microscopy investigation: The membrane complex in spermatogenesis of *Fenneropenaeus chinensis*. *Cytotechnology*, **56**(2), 113–121. doi: 10.1007/s10616-008-9132-5

Kangasniemi, M., Veromaa, T., Kulmala, J., Kaipia, A., Parvinen, M. and Toppari, J. (1990). DNA-flow cytometry of defined stages of rat seminiferous epithelium: Effects of 3 Gy of high-energy X-irradiation. *Journal of Andrology*, **11**(3), 312–317. doi: 10.1002/j.1939-4640.1990.tb03246.x

Kashiwabara, S., Kashimoto, N., Sanoh, S., Uesaka, T., Katoh, O. and Watanabe, H. (2003). Damage of the mouse testis by tritiated water and 137Cs-gamma-rays. *Hiroshima Journal of Medical Sciences*, **52**(3), 53–58.

Keane, T. J., Swinehart, I. T. and Badylak, S. F. (2015). Methods of tissue decellularization used for preparation of biologic scaffolds and *in vivo* relevance. *Methods*, **84**, 25–34. doi: 10.1016/j.ymeth.2015.03.005

Kerr, J. B., Savage, G. N., Millar, M. and Sharpe, R. M. (1993). Response of the seminiferous epithelium of the rat testis to withdrawal of androgen: Evidence for direct effect upon intercellular spaces associated with Sertoli cell junctional complexes. *Cell and Tissue Research*, **274**(1), 153–161. doi: 10.1007/BF00327996

Kim, Y., Selvaraj, V., Dobrinski, I., Lee, H., McEntee, M. C. and Travis, A. J. (2006). Recipient preparation and mixed germ cell isolation for spermatogonial stem cell transplantation in domestic cats. *Journal of Andrology*, **27**(2), 248–256. doi: 10.2164/jandrol.05034

Koruji, M., Movahedin, M., Mowla, S. J., Gourabi, H. and Arfaee, A. J. (2008). The morphological changes of adult mouse testes after ^{60}Co gamma-radiation. *Iranian Biomedical Journal*, **12**(1), 35–42.

Koruji, M., Movahedin, M., Mowla, S. J., Gourabi, H. and Arfaee, A. J. (2009). Efficiency of adult mouse spermatogonial stem cell colony formation under several culture conditions. *In Vitro Cellular and Developmental Biology. Animal*, **45**(5–6), 281–289. doi: 10.1007/s11626-008-9169-y

Lan, W., Nanshan, D. and Wei, L. (1999). Studies on spermiogenesis of a freshwater crab *Sinopotamon yangtsekiense* (Crustacea Decapoda). *Shui Sheng Wu Hsueh Bao = Acta Hydrobiologica Sinica*, **23**, 29–33.

Medina, A., García-Isarch, E., Sobrino, I. and Abascal, F. J. (2006). Ultrastructure of the spermatozoa of *Aristaeopsis edwardsiana* and *Aristeus varidens* (Crustacea, Dendrobranchiata, Aristeidae). *Zoomorphology*, **125**(1), 39–46. doi: 10.1007/s00435-005-0013-6

Mirzapour, T., Tengku Ibrahim, T. A. B., Movahedin, M. and Nowroozi, M. R. (2017). Morphological and ultrastructural studies of human spermatogonial stem cells from patients with maturation arrest. *Andrologia*, **49**(7), e12700. doi: 10.1111/and.12700

Mohaqiq, M., Movahedin, M., Mazaheri, Z. and Amirjannati, N. (2019). *In vitro* transplantation of spermatogonial stem cells isolated from human frozen–thawed testis tissue can induce spermatogenesis under 3-dimensional tissue culture conditions. *Biological Research*, **52**(1), 16. doi: 10.1186/s40659-019-0223-x

Parreira, G. G., Ogawa, T., Avarbock, M. R., França, L. R., Brinster, R. L. and Russell, L. D. (1998). Development of germ cell transplants in mice. *Biology of Reproduction*, **59**(6), 1360–1370. doi: 10.1095/biolreprod59.6.1360

Ramm, S. A., Schärer, L., Ehmcke, J. and Wistuba, J. (2014). Sperm competition and the evolution of spermatogenesis. *Molecular Human Reproduction*, **20**(12), 1169–1179. doi: 10.1093/molehr/gau070

Rodriguez-Sosa, J. R. and Dobrinski, I. (2009). Recent developments in testis tissue xenografting. *Reproduction*, **138**(2), 187–194. doi: 10.1530/REP-09-0012

Russell, L. D., Ettlin, R. A., Sinha Hikim, A. P. and Clegg, E. D. (1993). *Histological and histopathological evaluation of the testis*. In Wiley Online Library.

Schlatt, S., Kim, S. S. and Gosden, R. (2002). Spermatogenesis and steroidogenesis in mouse, hamster and monkey testicular tissue after cryopreservation and heterotopic grafting to castrated hosts. *Reproduction*, **124**(3), 339–346. doi: 10.1530/rep.0.1240339

Shokri, S., Hemadi, M. and Aitken, R. J. (2012). *Transmission electron microscopy for the quantitative analysis of testis ultra structure*. INTECH Open Access Publisher.

Somosy, Z. (2000). Radiation response of cell organelles. *Micron*, **31**(2), 165–181. doi: 10.1016/s0968-4328(99)00083-9

Sprando, R. L. (1990). Perfusion of the rat testis through the heart using heparin. In L. D. Russell, R. A. Ettlin, A. P. Sinha Hikim and E. D. Clegg (eds.), *Histological and Histopathological Evaluation of the Testis*. Cache River Press.

Stukenborg, J. B., Wistuba, J. W., Luetjens, C. M., Elhija, M. A., Huleihel, M., Lunenfeld, E., Gromoll, J., Nieschlag, E. and Schlatt, S. (2008). Coculture of spermatogonia with somatic cells in a novel three-dimensional soft-agar-culture-system. *Journal of Andrology*, **29**(3), 312–329. doi: 10.2164/jandrol.107.002857

Thakur, M., Gupta, H., Singh, D., Mohanty, I. R., Maheswari, U., Vanage, G. and Joshi, D. S. (2014). Histopathological and ultra structural effects of nanoparticles on rat testis following 90 days (Chronic study) of repeated oral administration. *Journal of Nanobiotechnology*, **12**, 1–13.

Tudge, C. C., Scheltinga, D. M. and Jamieson, B. G. M. (2001). Spermatozoal morphology in the "symmetrical" hermit crab. *Pylocheles (Bathycheles) SP.*(Crustacea, Decapoda, Anomura, Paguroidea, Pylochelidae)', *Zoosystema*, **23**, 117–130.

van der Horst, G., Kotzé, S. H., O'Riain, M. J. and Maree, L. (2019). Testicular structure and spermatogenesis in the naked mole-rat is unique (degenerate) and atypical compared to other mammals. *Frontiers in Cell and Developmental Biology*, **7**, 234. doi: 10.3389/fcell.2019.00234

Van Pelt, A. M. M., Morena, A. R., van Dissel-Emiliani, F. M. F., Boitani, C., Gaemers, I. C., De Rooij, D. G. and Stefanini, M. (1996). Isolation of the synchronized A spermatogonia from adult vitamin A-deficient rat testes. *Biology of Reproduction*, **55**(2), 439–444. doi: 10.1095/biolreprod55.2.439

Villagra, L. I., Ramos, I., Cisint, S., Crespo, C. A. and Fernández, S. N. (2018). Electron microscopy observations on testis and spermatozoa of *Leptodactylus chaquensis* (Anura, Leptodactylidae). *Micron*, **105**, 35–46. doi: 10.1016/j.micron.2017.11.007

Watson, M. L. (1952). Spermatogenesis in the albino rat as revealed by electron microscopy; a preliminary report. *Biochimica et Biophysica Acta*, **8**(4), 369–374. doi: 10.1016/0006-3002(52)90060-7

Xianjiang, K. and Suo, W. (2000). Studies on the changes of morphology and structure of the spermatozoon in *Penaeus chinensis*. *Donghai Marine Science*, **18**, 40–46.

https://doi.org/10.1017/S096719942300062X Published online by Cambridge University Press